

NASA-CR-203228

Two-point correlation measurements in a recovering turbulent boundary layer

Srba Jovic

Eloret Institute/NASA Ames Research Center, MS 229-1, Moffett Field, CA 94035-1000

Abstract

Space-time correlation and the shear stress conditional quadrant decomposition techniques were used to assess the structure of a turbulent boundary layer. The boundary layer was recovering from the strong perturbation produced by a backward-facing step. All two-point, two-component, velocity measurements were conducted 38 step-heights, h , downstream from the step. It is found that the structure of the recovering boundary layer is dominated by an attached double-cone eddy in the near wall region and by a double-roller eddy in the outer flow. The postulated structure is more elongated in the cross coordinate directions of the recovering boundary layer when compared to the one found in a regular flat-plate zero-pressure gradient turbulent boundary layer. The conditional quadrant analysis have revealed that the shear stress production is dominated by the Q_2 and Q_4 events while the contribution by the interactive events, Q_1 and Q_3 , remains relatively small. It appears that the Q_1 and Q_3 motions are largely induced by the very energetic Q_2 and Q_4 events.

1. INTRODUCTION

Two-point correlation measurements have proven to be a very powerful tool in the analysis and quantification of organized structures in turbulent flows. There are basically two schools of thought about how to use two-point measurements for deduction of organized structures. One approach, deductive in nature, checks the consistency of a proposed organized structure with measured two-point correlation profiles. Townsend (1956,1976) was the first to demonstrate this approach using Grant's (1958) two-point measurements in the turbulent wake behind a circular cylinder and in the flat-plate turbulent boundary layer (TBL). The results of this technique were revolutionary at a time, when they gave birth to the concept of the double-roller eddy structure in the wake flow and the attached eddy in the TBL. The second, inductive, approach has been introduced by Lumley (1967). He proposed the proper orthogonal decomposition (POD) technique to objectively identify and extract the organized structure of a turbulent flow. This method uses an orthogonal decomposition to obtain eigenmodes from two-point correlation profiles. An organized structure is identified as the most energetic eddy and is uniquely defined as the eigenfunction with the largest eigenvalue. These eigenfunctions can be subsequently used to reconstruct an associated flow structure and obtain its contribution to the Reynolds stress tensor. Using the POD tech-

nique, Payne (1966) utilized Grant's (1958) two-point measurements to find that the dominant structure in a turbulent wake is the double-roller eddy. Bakewell & Lumley (1967) utilized the POD to obtain a pair of counter rotating eddies in the wall region of the turbulent pipe flow. Both findings are consistent with Townsend's (1956,1976) proposed structural models.

The objective of this investigation is to deduce the flow structure of a recovering turbulent boundary layer using two-point two-component velocity measurements based on their similarity with the measurements of Grant (1958) and Tritton (1967). In addition, new potentials of two-point measurement are exploited using quadrant decomposition and conditional quadrant decomposition of the shear stress.

2. EXPERIMENTAL ARRANGEMENT AND CONDITIONS

The experiment was performed in the 20x40cm low-speed open-circuit wind tunnel at the NASA Ames Research Center. The boundary layer was tripped at the end of the contraction to promote regular transition. The fully developed turbulent boundary layer was perturbed 169cm downstream from the trip by a backward-facing step of the height, h , of 38mm. The aspect ratio W/h , where W is the wind tunnel width, was 11 while the duct area expansion ratio was 1.19. The reference velocity, U_{ref} , measured at a reference point upstream of the step was 10.0m/s which corresponded to a Reynolds number based on the step-height, R_h , of 25500. The free stream turbulence level in the tunnel was 0.4% measured at 10.0m/s. The boundary layer thickness, $\delta \equiv \delta_{99}$, upstream of the step was 30mm which yielded $\delta/h=0.77$ with a Reynolds number based on the momentum thickness, R_θ , of 2000. The separated flow reattaches at $6.7h$ downstream from the step. The free stream velocity, U_e , of the recovering boundary layer at $x/h=38$ was 8.9 m/s, the boundary layer thickness, δ , was 110 mm, the momentum thickness, θ , was 12 mm, the shape factor, H , was 1.3 and the Reynolds number, R_θ , was 7100.

Turbulence measurements were performed with a set of constant-temperature anemometers used in conjunction with X-wire probes. The sensor filaments were made of 10% Rhodium-Platinum wire, 2.5 μ m in diameter and 0.6mm long, which resulted in an aspect ratio, l/d , of 240 and normalized length, $l^+ = l u_\tau / \nu$, of 14.5. The frequency response of the constant-temperature anemometer was 50kHz. Data were collected by a microVax II computer interfaced with a high speed sample-and-hold Tustin A/D converter which was set at 6000 Hz. The record length of each channel was 30 sec.

Instantaneous turbulent velocity fluctuations u and v were measured in the streamwise, x , and normal, y , directions respectively. The z -axis is in the spanwise direction of the flow. The subscripts 1, 2, 3, will also be used to refer to the x , y and z directions respectively.

3. RESULTS AND DISCUSSION

3.1 Mean flow characteristics

All the measurements were performed at a fixed streamwise location $x/h=38.55$.

The two dimensionality of the mean flow was checked by the spanwise measurements of the mean velocity component, U , and the shear-stress coefficient C_f . It was found that the velocity distribution was uniform in the z -direction to $\pm 2\%$ measured at $y/\delta = 0.45$ while C_f distribution was uniform to $\pm 4\%$ for $-\delta$ to δ about the symmetry plane of the tunnel.

The wall stress was measured directly using laser oil interferometry. The measured skin friction coefficient, $C_f = 0.003$, was used to normalize the mean streamwise velocity. It was compared against the universal law-of-the-wall velocity distribution, $U^+ \equiv U/u_\tau = 1/0.41 \ln y^+ + 5.1$, shown in Figure 1(a). It appears that the velocity distribution agrees well with the logarithmic velocity distribution in the near-wall region up to $y^+ = u_\tau y/\nu$ of about 200 or $y/\delta = 0.08$. However, it dips below the universal log-law distribution for greater values of y^+ . This resulted in the larger value of Prandtl's mixing length in the outer part of the recovering boundary layer, and in the larger slope in the inner layer. Cutler & Johnston (1989), Jovic & Browne (1990) and Jovic (1993) have observed values of the mixing length in the outer layer which are about two times larger than those in a regular TBL.

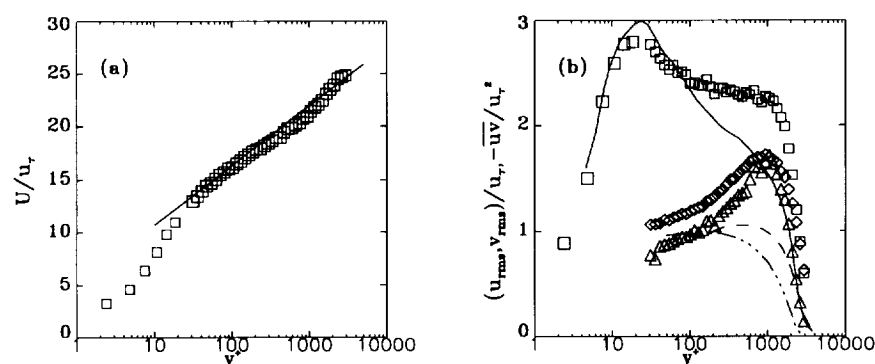


Figure 1. (a) Mean velocity profile and (b) turbulence intensities and shear stress. Symbols: (a) —, $U^+ = 1/0.41 \ln y^+ + 5.1$, (b) \square , u_{rms}/u_τ ; \triangle , v_{rms}/u_τ ; Δ , $-\overline{uv}/u_\tau^2$. Klebanoff's experiment: —, u_{rms}/u_τ ; - - -, v_{rms}/u_τ ; ... —, $-\overline{uv}/u_\tau^2$.

Turbulence intensities u_{rms} and v_{rms} and the shear stress, $-\overline{uv}$, profiles are shown in Figure 1(b). It appears that the streamwise turbulence, u_{rms} , agrees well with Klebanoff's (1954) measurements in the inner layer. Using the transport equation of the turbulent kinetic energy, Jovic (1993) showed that the near-wall structure of this flow has nearly recovered to an equilibrium state at this x location unlike the outer part of the flow. It was further shown that the structure in the near-wall and the outer flow regions have different rates of recovery. The near-wall structure recovers much faster and attains a quasi-equilibrium state for $x/h > 30$ while the outer turbulent structure takes presumably $100h$ to recover to a flat-plate TBL structure.

3.2 Results of correlation measurements

Correlation between two quantities p and q at two spatial points \mathbf{x} and $\mathbf{x}+\mathbf{r}$ is defined as

$$R_{pq}(x, r) = \frac{\overline{p(x)q(x+r)}}{\sqrt{\overline{p^2(x)}}\sqrt{\overline{q^2(x)}}}$$

where \mathbf{x} denotes the position vector of the fixed (or reference) probe and \mathbf{r} is the separation vector. The first subscript, p , in R_{pq} denotes a quantity at a reference point and the second one, q , denotes a quantity at a location of the moving probe. Four different correlations were considered, i.e. $R_{uu}(\mathbf{x}, \mathbf{r})$, $R_{vv}(\mathbf{x}, \mathbf{r})$, $-R_{uv}(\mathbf{x}, \mathbf{r})$ and $-R_{vu}(\mathbf{x}, \mathbf{r})$. The present discussion will be confined to cases where the separation vector was $\mathbf{r} = (0, r_2, 0)$ or $(0, 0, r_3)$, i.e. when the moving probe is moved in the normal, y , or spanwise, z , direction keeping the streamwise location, x , constant and equal to that of the stationary probe. In this case the notation can be abbreviated to $R_{pq}(r_2)$ and $R_{pq}(r_3)$ respectively. Note that $R_{pq}(0)$ is equal to unity in the case when $p \equiv q$ and to the local correlation coefficient when $p \neq q$. Any departure from these values can be attributed to a finite initial displacement of probes. Measurements were performed for four different y locations of the stationary probe, namely $y/\delta = 0.012, 0.2, 0.38$ and 0.75 ($y^+ = 30, 510, 965$ and 1905 respectively). The stationary probe was located at $z/\delta = 0.45$ off the plane of symmetry of the tunnel for all z traverses. For the z traverse in the wall region, the stationary probe was moved to a slightly larger distance from the wall, namely, to $y/\delta = 0.018$ ($y^+ = 45$). Two y/δ locations, 0.012 and 0.38 , were selected because $\overline{u^2}$ attains a maximum (or nearly a maximum) values at these locations in the inner and the outer layers of the recovering boundary layer.

Correlations $R_{uu}(r_2)$, $R_{vv}(r_2)$, $-R_{uv}(r_2)$ and $-R_{vu}(r_2)$ for different distances from the wall are shown in Figure 2. All four correlations are virtually non-negative for r_2 separations. The correlation $R_{uu}(r_2)$ for $y/\delta = 0.012$ remains non-zero for very large r_2 separations approaching zero value at about $r_2/\delta = 0.85$ as seen in Figure 2(a). For the same distance of the reference probe from the wall, $R_{uu}(r_2)$ decays rapidly for small r_2 suggesting the presence of structures of smaller length scales near the wall. The extent of the strong correlation over larger r_2 separations implies presence of unusually large structures in the outer part of the flow which appear to communicate with the near-wall flow structure. It appears that $R_{uu}(r_2)$ for the two different distances from the wall, $y/\delta = 0.20$ and 0.38 , are identical for positive r_2 (see Fig. 2(a)), suggesting that length scales in the outer layer are constant. However, the correlation falls off rapidly for negative r_2 , particularly when the stationary probe is closer to the wall. For the stationary probe located at $y/\delta = 0.012$, $R_{vv}(r_2)$ decreases rapidly in the y direction, falling to a value of almost zero at $r_2/\delta = 0.2$ and remaining virtually zero for the rest of the boundary layer. For larger distances of the stationary probe from the wall, $R_{vv}(r_2)$ exhibit surprisingly high magnitudes suggesting that motions associated with the v fluctuating component are of much larger length scales than those found in the flat-plate TBL of Grant (1958) and Tritton (1967). It appears that $R_{vv}(r_2)$ is identical for positive r_2 (see Fig. 2(b)) for the two characteristic positions of the reference probe ($y/$

$\delta=0.20$ and 0.38) as in the case of $R_{uu}(r_2)$. Reduced size of structures near the wall leads to a rapid decay of $R_{vv}(r_2)$ for negative r_2 . Comparison of $R_{uu}(r_2)$ and $R_{vv}(r_2)$ with classic measurements of Grant (1957) and Tritton (1967) (not shown) shows that u and v fluctuating components are strongly correlated over much larger r_2 separations in the present experiment than in the case of a regular TBL. It appears that the length scales of the recovering boundary layer at the given x location are roughly two times larger than those of a flat-plate TBL. Correlations $-R_{uv}(r_2)$ and $-R_{vu}(r_2)$ are not identical for y traverses as seen from Fig. 2(c) and (d). However, they should be identical for $r_2=0$ and the reason why they are not is because of the finite initial spanwise separation of the two probes. The correlation $-R_{vu}(r_2)$, for $y/\delta=0.012$, decays rapidly for increasing r_2 separations, approaching zero at about $r_2/\delta=0.45$. For larger distances from the wall $-R_{vu}(r_2)$ falls less dramatically showing that u and v are well correlated further from the wall.

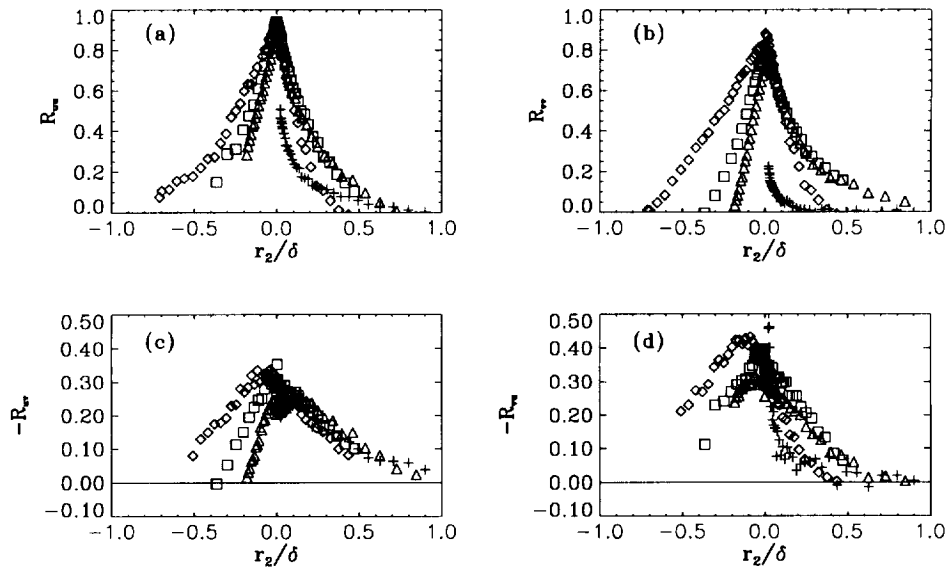


Figure 2. Space correlations for r_2 separations for four different y locations of stationary probe. Symbols: +, $y/\delta=0.012$; Δ , $y/\delta=0.20$; \square , $y/\delta=0.38$; \diamond , $y/\delta=0.75$.

Figure 3 shows four correlations for r_3 separations for the four different distances of the reference probe from the wall. The most striking point observed in their behavior is the change of the sign. The change of the sign suggests periodicity in the z direction. The separation at which the minimum of the $R_{uu}(r_3)$ profile occurs provides an estimate of an average separation between the high and low speed fluid. Near the wall (reference probe was at $y/\delta=0.018$), $R_{uu}(r_3)$ decreases rapidly for $r_3/\delta<0.05$ indicating the presence of motions of much smaller scales than those for the larger distances from the wall (Fig.3(a)). However, the rate of decay of $R_{uu}(r_3)$ reduces for separations $r_3/\delta>0.05$ eventually falling off to zero

value at $r_3/\delta=0.35$. This two-component form of the correlation profile close to the wall according to Townsend (1956) suggests the presence of two distinct ranges of eddy sizes. Minimum values of R_{uu} occur at about $r_3/\delta=0.6$ for the reference probe at $y/\delta=0.20$ and 0.38 and at $r_3/\delta=0.7$ for $y/\delta=0.75$. Apparently the spanwise spacing of the high/low speed streaks gradually increases with the normal direction. Close to the wall, $R_{vv}(r_3)$ becomes negative for r_3 which are smaller than those of the other correlations. The negative values of $R_{vv}(r_3)$, together with the occurrence of the minimum, suggest the presence of streamwise vortical structures. The negative lobe of R_{vv} almost disappears away from the wall for $y/\delta>0.38$. The separation of the minimum from the origin can be interpreted as an average diameter of a characteristic streamwise vortex. The R_{vv} , $-R_{uv}$ and $-R_{vu}$ correlations close to the wall decrease very rapidly so that due to the lack of the spatial resolution in this region the decreasing limbs of the correlation functions have not been properly resolved.

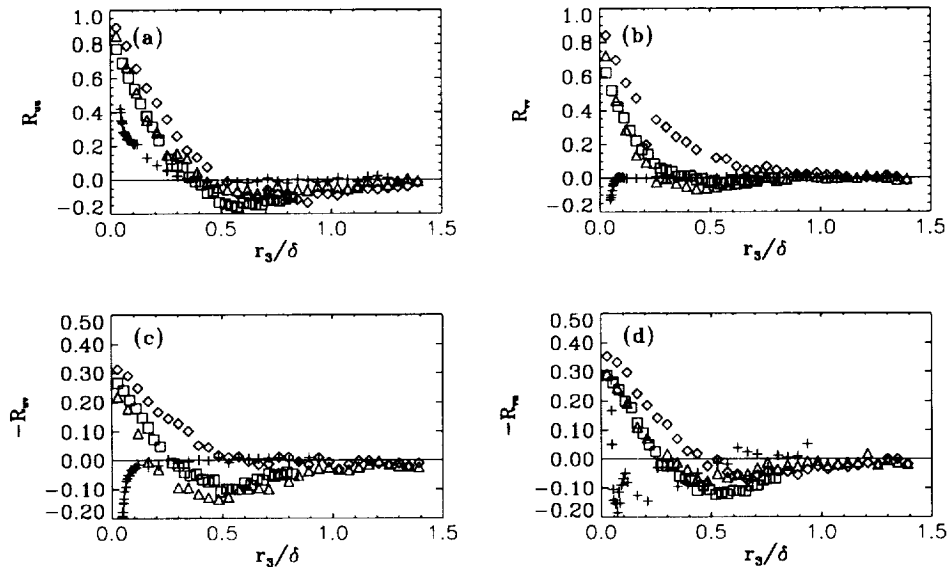


Figure 3. Space correlation for r_3 separations for four different y locations of stationary probe. Symbols: +, $y/\delta=0.018$; Δ , $y/\delta=0.20$; \square , $y/\delta=0.38$; \diamond , $y/\delta=0.75$.

Measured space correlations are similar to those measured in a flat-plate turbulent boundary layer by Grant (1958) and Tritton (1967). However, the turbulent quantities of this flow correlate over greater spatial separations in both y and z directions suggesting that there are larger scales of motion in this flow than in a flat-plate TBL. This provides indirect evidence that the large scale organized structures present in the recovering boundary layer are similar to the Townsend's attached double-cone and double-roller eddies in the near-wall and outer layers respectively, however, with larger y and z dimensions. The two characteristic

structures can be connected to form a hairpin structure as shown in Figure 5. Space-time correlations will lend some more evidence in favor of the above hypothesis.

Space-time correlations for the stationary probe located near the wall at $y/\delta=0.012$ are shown in Figure 4. The phase shift seen in $R_{uu}(r_2, \tau)$ increases as the moving probe moved away from the wall. Favre, Gaviglio & Dumas (1957) were the first ones to observe the same phenomenon in their two-point space-time correlation measurements. Their measurements were consistent with Grant's (1958) outward moving "jets" of his large eddy model. Brown and Thomas (1977), using an array of hot wires and wall shear stress probes, have shown that this increasing time delay with distance from the wall is due to the presence of the large coherent structures spanning an entire boundary layer at an inclined angle. This is consistent with the findings of Head & Bandyopadhyay (1981) who have observed hairpin vortical structures in the outer region of a boundary layer using a flow visualization technique. Using the conditional sampling technique, Jovic & Browne (1989) have shown the presence of the inclined δ -structure in the reattached turbulent boundary layer at $x/h=17$ of the same backward-facing step flow. They have interpreted this structure as a hairpin like vortex. There is a striking difference between $R_{uu}(r_2, \tau)$ and $R_{vv}(r_2, \tau)$ (see Fig. 4(b)). It is normally expected that one would observe a time delay in all space-time correlations due to the intermittent passage of large organized motions which span the flow at an angle relative to the wall. Instead, the $R_{vv}(r_2, \tau)$ shows no time shift for different r_2 separations.

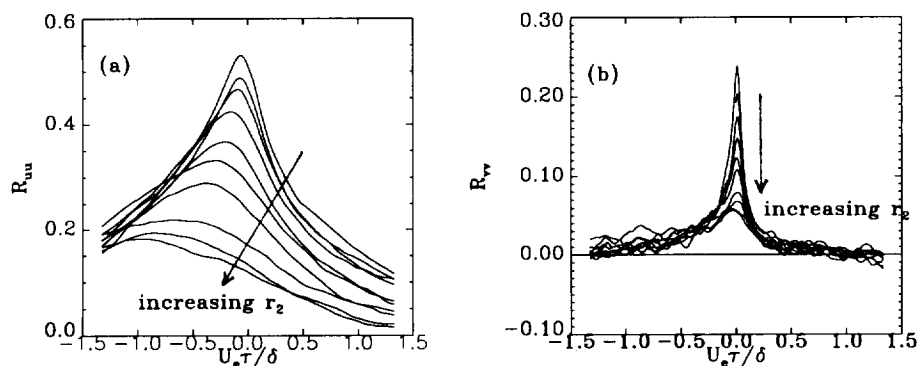


Figure 4. Space-time correlation for r_2 separations for stationary probe at $y/\delta=0.012$.

Observed time delays of the maximum space-time correlations for different r_2 separations (Fig. 4(a)) can be used to reconstruct the spatial form of the detected energetic structure across the boundary layer. It is well accepted that a structure is convected at a nearly constant speed across an entire boundary layer thickness. The convection velocity is approximately $U_c=0.8U_e$. A possible qualitative model of an organized structure in the recovering TBL is presented in Figure 5. Taylor's

hypothesis of “the frozen turbulence” and the convection velocity, U_c , were used to determine the angles of the postulated structure with respect to the x -axis. The obtained angle in the near-wall, high shear, region is in the range of $\phi_1=15^\circ$ to 20° which agrees remarkably well with angles obtained by other experimentalists. In the outer layer, the angle is in the range of $\phi_2=40^\circ$ to 70° which is somewhat larger than those for a flat-plate TBL. It is deduced that the blending between the two layers occur in the region of $y/\delta \approx 0.2$. The proposed model of the organized structure in the recovering TBL is shown in Figure 5. Based on the two-point space-time correlations, R_{pq} , for r_2 and r_3 separations of the moving probe, presented above, and on their similarities with the results of the cited experiments, it was deduced that the dimensions of the postulated structure are about two times larger in the normal and the spanwise directions than that of the flat-plate TBL.

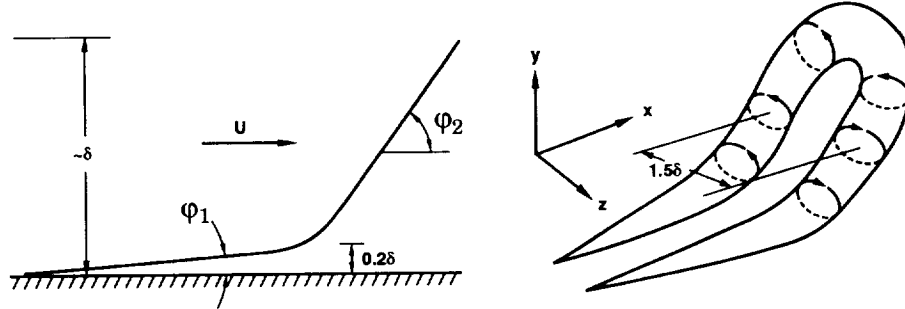


Figure 5. Proposed model of the organized structure in the recovering TBL.

3.3 The conditional quadrant analysis of the shear stress

Simultaneous two-point measurements were used for the conditional quadrant analysis of the shear stress which can lead to a better understanding of the production mechanisms in TBLs.

The conditional probability that the event, Q_i ($i=1,2,3,4$) at the location of the moving probe occurs given that the event Q_j ($j=1,2,3,4$) has occurred at the stationary point is defined as

$$P_{ij} = P(Q_i \cap Q'_j) / P(Q'_j)$$

and the associated conditional quadrant contribution of the Reynolds shear stress at a moving point is denoted as $\langle uv \rangle_{ij} / \overline{uv}$ corresponding to a Q_{ij} event. For example, if a Q_2 event is observed at the stationary point of a two-point measurements there are four possible events which may occur at the location of the moving point, i.e. shear stress can be in either of the four quadrants.

Hence, the probability, P_{i2} , of Q_i given that the Q_2 has occurred at a given fixed point is obtained together with the associated $\langle uv \rangle_{i2} / \overline{uv}$ where $i=1,2,3,4$. A conditional quadrant decomposition is shown in Figure 6 for the fixed probe at $y^+=30$ ($y/\delta=0.012$). As can be seen from Figure 6, the conditional interactive motions, Q_{1i} and Q_{3i} , are relatively weak and spatially limited. It appears that the interactive motions are independent of the condition at the reference probe for $y/\delta > 0.2$. However, Q_{14} and Q_{32} motions near the wall appear to be well correlated with Q_4 and

Q_2 respectively (Figs 6(a),(c)). In other words, Q_4 events might produce Q_1 events in the wall region by the “splat” effect which eventually leads to the formation of streamwise vortices and a Q_2 events as argued by Moin & Kim (1982) and Kim (1983). In addition, Q_3 interactive motions in the wall region might be due to the deflection of ejections which produce Q_2 events. A dramatic change in the contributions to the shear stress by the different quadrants is observed when Q_2 and Q_4 are chosen as conditions at the reference probe near the wall (Figs 6(b),(d)). The positive $\langle uv \rangle_{22}/\overline{uv}$ conditional contribution at the moving probe initially falls off rapidly for $y/\delta < 0.1$ (Fig. 6(b)). The $\langle uv \rangle_{42}/\overline{uv}$ contribution is consistently smaller across the entire boundary layer, while interactive motions exhibit increased contribution in the vicinity of the stationary probe. The $\langle uv \rangle_{44}/\overline{uv}$ contribution falls off rapidly (Fig. 6(d)) for $y/\delta < 0.1$ while it decrease gradually for larger r_2 separations becoming smaller than $\langle uv \rangle_{24}/\overline{uv}$ for $y/\delta > 0.35$.

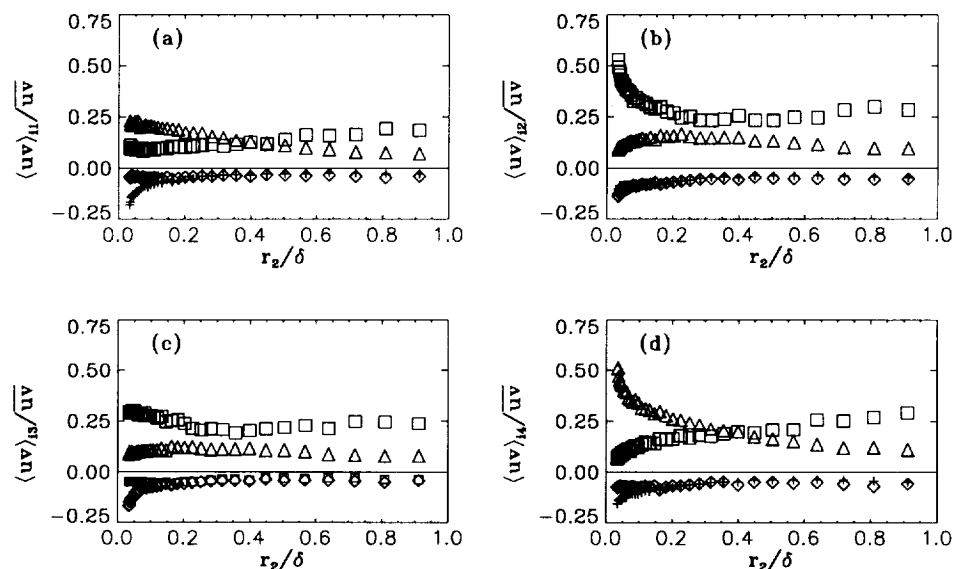


Figure 6. Conditional contribution of different quadrants to the shear stress providing that: (a) Q_1 has occurred at the fixed probe location $y/\delta=0.012$, (b) Q_2 , (c) Q_3 , (d) Q_4 . Symbols: +, Q_1 ; □, Q_2 ; ◇, Q_3 ; △, Q_4 .

It appears that the negative contribution, $\langle uv \rangle_{14}/\overline{uv}$, increases for small values of y giving support for the “splat” effect. The analysis of the conditional quadrant contribution was performed for an instantaneous velocity field at two points in space. However, having in mind that the postulated structure is a 3-D structure inclined in the streamwise direction, a similar analysis is now under way using a time shift between signals at two different spatial locations.

4. CONCLUSIONS

The structure of the recovering turbulent boundary layer perturbed by a backward-facing step was investigated experimentally using two-point two-component velocity measurements. General similarity of the measured spatial correlations with those of Grant (1957) and Tritton (1967) suggested that the characteristic structure is similar to the attached eddies in the near-wall layer and to the double-roller eddy in the outer layer as proposed by Townsend (1976). The two characteristic structures present in TBLs can be connected into a hairpin structure as supported by many other studies. The observed organized structure of the recovering boundary layer appears to have larger dimensions in the two cross flow directions when compared to an undisturbed flat plate TBL. The conditional quadrant analysis of the shear stress suggests that Q_2 and Q_4 are dominating mechanisms in the recovering TBL. In addition, it appears that the interactive motions, Q_1 and Q_3 , are produced by the "splatting" of sweep motions and deflection of ejection motions respectively.

ACKNOWLEDGEMENTS

This research was supported by NASA Grant NCC2-465 which is gratefully acknowledged. The hospitality of S. Davis and help by the FML staff are gratefully acknowledged.

5. REFERENCES

1. Bakewell, H and Lumley, J.L. 1967 *The Physics of Fluids*, Vol. **10**, No. 9.
2. Brown, L.G. and Thomas, A.S.W. 1977 *The Physics of Fluids*, Vol. **20**, No. 10, Part II, S243.
3. Favre, A.J., Gaviglio, J.J. and Dumas, R. 1957 *J. Fluid Mech.* **2**, 313.
4. Grant, H.L. 1958, *J. Fluid Mech.*, **4**, 149.
5. Head, M.R. and Bandyopadhyay, P. 1981 *J. Fluid Mech.*, **107**, 297.
6. Jovic, S. and Browne, L.W.B. 1989, *Tenth Australasian Fluid Mechanics Conference*, University of Melbourne, Melbourne, December 11-15.
7. Jovic, S. and Browne, L.W.B. 1990 *Engineering Turbulence Modelling and Experiments Proceedings of the International Symposium on Engineering Turbulence Modelling and Measurements*, September 24-28, Dubrovnik, Yugoslavia, ed. W. Rodi and E.N. Ganic.
8. Jovic, S. 1993 *2nd International Symposium on Engineering Turbulence Modelling and Measurements*, May 31- June 2, Florence, Italy (to appear).
9. Kim, J. 1983 *Phys. Fluids*, Vol. **26**, No. 8.
10. Klebanoff, P.S. 1954 National Advisory Committee for Aeronautics, TN. 3178.
11. Lumley, J.L. 1967 *Proceedings of the International Colloquium on the Atmosphere and its Influence on the Radio Wave Propagation* (Doklady Akademia Nauk SSSR, Moscow).
12. Moin, P. and Kim, J. 1982 *J. Fluid Mech.*, **118**, 341.
13. Townsend, A.A. 1976 (and 1956) *The Structure of the Turbulent Shear Flow*. Cambridge University Press.
14. Payne, F.R. 1966 *PhD Thesis*, Pennsylvania State University, University Park.